Graphene Oxide-Aryl Substituted Triazole Thin Hybrid Corrosion Resistant Coating for Copper

Nasima Arshad,[1*] Muhammad Imran[1], Muhammad Akram[1] and Fouzia Altaf[2]

[1]*Department of Chemistry, Allama Iqbal Open University, Islamabad, 44000 Pakistan*
[2]*Pakistan Council of Research in Water Resources, Ministry of Science and Technology, Islamabad, 44000 Pakistan*

[*]Corresponding author: nasimaa2006@yahoo.com; nasima.arshad@aiou.edu.pk

Received 23/03/20; accepted 05/08/2021
https://doi.org/10.4152/pea.2022400304

Abstract

A graphene oxide-triazole hybrid anti-corrosive coating was done by fabricating a triazole derivative – 2-(5-mercapto-4-((3-nitrophenyl)amino)-4H-1,2,4-triazol-3-yl)isoindoline-1,3-dione (4-NBT) on a graphene oxide (GO) coated Cu electrode. The GO-4-NBT hybrid coating effect on the Cu surface corrosion behavior was electrochemically monitored through cyclic voltammetry (CV), potentiodynamic polarization (PDP) and electrochemical impedance spectroscopy (EIS). The fabrication of a protective coating was done in two steps. Firstly, GO was electrochemically deposited on the Cu electrode in two different aggressive media (1 M HCl and 0.1 M Na_2SO_4), separately. Secondly, different 4-NBT concentrations were employed to reinforce GO corrosion resistant properties. CV studies revealed that GO-4-NBT effectively suppressed the metal oxidation and oxygen reduction. EIS studies suggested that the electrochemical process on the Cu surface with GO and GO-4-NBT was charge transfer controlled. The corrosion inhibition efficiency (IE) measured by PDP and EIS was enhanced with a related raise in 4-NBT concentration. Electrochemical studies revealed that the GO-4-NBT was a mixed type of inhibitor that predominantly inhibited the anodic reaction, especially in the case of 0.1 M Na_2SO_4. Adsorption studies further indicated the involvement of a stable and spontaneous adsorption mechanism, most probably by chemisorption. GO-4-NBT has shown significant corrosion protection activity in 0.1 M Na_2SO_4.

Keywords: GO-4-NBT, Cu electrode, anti-corrosion coating, electrochemical studies by, PDP and EIS, and adsorption studies.

Introduction

Cu is recognized as one of the most versatile engineering materials, due to its thermal and electrical conductivity, corrosion resistance and reasonable mechanical properties. It is widely used for building constructions, industrial machinery, water-cooling systems, desalination plants and heat exchangers. However, Cu applications have been limited, due to its chemically reactive nature. Cu forms oxide films of various kinds, depending on the nature of the environment it is exposed to. Salts can also be thought about as major contributor. Chloride ion (Cl^-), being a

robust reducing agent, speeds up corrosion by reacting at the substrate surface as a catalyst, to accelerate the corrosion process [1]. Another cause is the exposure to aggressive media, such as hydrogen chloride (HCl) and Nitric acid (HNO_3), which are extensively employed in several chemical industries [2]. Thereby, the development of an efficient and durable anti-corrosion protective coating is essential for its use in the above applications [3].

Conventional organic, inorganic and metallic anticorrosive coatings have been developed to protect metals from corrosion [4, 5]. The inhibitors efficiency is mostly related to the presence of polar functional groups with heteroatoms such as S, O or N and pi (π) electrons in their compounds [6, 7]. These polar groups in the molecules provide strong protection by adsorbing onto the metallic surfaces through π- and non-bonding electrons, polar groups and aromatic rings, and blocking one or more of the corrosion reactions occurring at the solution/metal interface [8, 9]. However, traditional corrosion resistant coatings have disadvantages, such as the use of volatile organic compounds or a high pigment volume concentration, which have created environmental hazards. Hence, a natural polymer such as chitosan and its derivatives could be considered as an attractive alternative to organic corrosion inhibitors, as it shows significant interacting capability with metals, via $–NH_2$ groups available on its chain [10]. In addition, these anti-corrosion coatings are believed to alter Cu attractive electrical and thermal properties [11], minimize the disadvantages of traditional coatings, and to be long lasting environmentally friendly compounds, at the same time not interfering with the material characteristic properties. Nanostructure materials have made it possible [12].

Carbon-based nanomaterials have been chosen due to some valuable features, such as an impressive chemically stabilization, low thermal coefficient, extraordinary thermal conductivity, high lubricity, lightness, porous surface, non-toxicity, resistance to radiation, being highly recommended for green chemistry application and friendly to organisms [13].

Graphene is comparatively new and has attracted significant interest, due to its unique combination of properties that are ideal for corrosion inhibiting coatings. It is a two-dimensional, single atom, thick honeycomb crystal lattice of carbon allotrope formed by tightly packed sp^2 carbon atoms. Because of the free electrons, it has exceptionally high electrical and thermal conductivity, strength and ductility [14, 15]. It is chemically inert, stable in an ambient atmosphere up to 400 ºC, and it can be grown on a meter-scale, and mechanically transferred onto arbitrary surfaces [14]. Since single-layer and multilayer graphene films are exceptionally transparent (>90% transmittance for 4-layered graphene) [15, 16], they do not perturb the underlying metal optical properties. Yet, direct graphene deposition on the metal surface is a major challenge while working with it. In addition, it has poor dispersion in both aqueous and non-aqueous solvents [15]. In chemical vapor, deposited graphene on Cu shows some disparities in corrosion resistance, due to irregularities, cracks, domain boundaries, wrinkles and folds in the protective layer [16].

Contrarily, graphene oxide (GO) has a lamellar structure, with both sp^2 and sp^3 hybridized carbon atoms forming a hexagonal carbon network. On its basal plane, GO has a greater number of exposed oxygen atoms containing functional groups, such as epoxide and hydroxyl and, on the edges, it has carbonyl and carboxyl groups which make it appropriate for bonding with both organic and inorganic materials by other forces than those of full covalent bonds. Both hydroxyl and epoxide groups make GO a better material than graphene, in terms of hydrophilicity and ease of dispersion in water, and of its ability to form hybrids and polymers [15, 16].
Therefore, considering the GO significance in varied applications in current years, this study focused on the fabrication of a GO-4-NBT hybrid protective coating for a Cu electrode, by electrochemical deposition. Further, based on electrochemical findings, GO-4-NBT anticorrosive activity on the Cu surface in 1 M HCl and 0.1 M Na_2SO_4 aggressive media was explored. The 4-NBT structure is given in Fig.1.

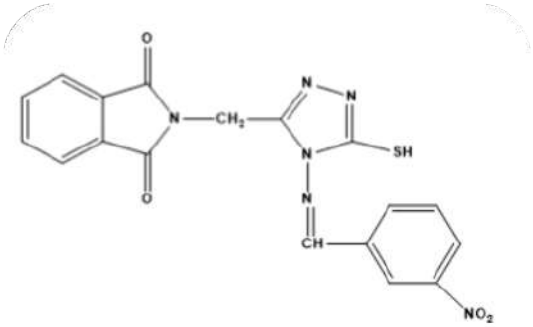

Figure 1. 4-NBT structure.

Experimental

Working electrode preparation

AISI 10100 Cu (99.99%) was chopped into circular discs in a die cutting machine. Electrical connections were made possible by a soldering process. After embedding into a Teflon tube, the exposed surface (with an area of 1.0 cm^2) was abraded with various grit size emery papers (i.e., 800, 1200, 2000 and 4000). The smooth surface was further degreased with acetone, ultra-sonicated for 3 min, systematically rinsed with distilled water and then dried in air.

Chemicals and solution preparation

All chemicals used were commercially available and of analytical grade. Graphite powder, with a purity of 99%, was used to prepare GO, by employing Hummer's technique [17, 18]. 2 g of graphite powder were mixed with 1 g of sodium nitrate ($NaNO_3$), followed by the addition of 46 mL of concentrated sulfuric acid (H_2SO_4), under constant stirring. After 1 h, 6 g of the potassium permanganate ($KMnO_4$) oxidizing agent were added to the solution, with vigorous stirring, at a temperature below 15 ºC, to avoid explosion. The mixture was constantly stirred for 15 h, at 35 ºC, and the resulting brownish paste was diluted by adding 500 mL of distilled water, with

vigorous stirring. Finally, 10 mL of hydrogen peroxide (H_2O_2) (30%) were slowly added to the mixture, after which the color of the latter changed to bright yellow. Then, it was centrifuged and washed with HCl and distilled water, sequentially, to remove the residual ions. Further, the end product was kept in vacuum desiccators at room temperature, in order to dry it prior to use. A GO dispersion of 1 mg/mL was prepared by ultra-sonication for 30 min. From the 4-NBT (5.0×10^{-3} M) stock, two dilutions were made, 0.05 and 0.1 mM, in dimethyl sulfoxide (DMSO).

Instrumentation

Electrochemical studies of the Cu surface were carried out by using an "AUTOLAB" PGSTAT-302 potentiostat/galvanostat, with GPES (General Purpose Electrochemical System) and FRA-2 modules, and a software package version 4.9 (Eco Chemie, Netherland). For CV and PDP measurements, a GPES module, and, for impedance studies, a FRA-2 module, were separately run. The pH values were adjusted with a pH meter (Jenway, 3510 model). An analytical balance (Shimadzu AUW 320 model) was used to weigh the Mg/mol of the samples.

Electrochemical procedure

An electrochemical cell with three electrode configurations was used for redox (reduction/oxidation) measurements. A Cu disc (area of 1 cm^2), a Pt wire and saturated calomel (SC) were used as working, counter and reference electrodes, respectively. The SCE was placed in a lugging capillary, and the tip was kept closer to the working electrode (WE) exposed surface, so that the IR (voltage) drop could be minimized. All electrochemical experiments were carried out using freshly prepared, clean and dried WE surfaces in aerated unstirred solutions, at 298 K. CVs of the bare Cu-electrode in 0.1 M Na_2SO_4 and 1 M HCl solutions were recorded, separately, vs. SCE, within a potential scan range from 1 V to -1.5 V. Then, CV responses of the Cu electrode were recorded with 1 mL of 1mg/mL GO dispersion, and, afterwards, with 0.05 and 0.1 mM of GO-4-NBT. The scan rate was adjusted at 50 mVs^{-1} for each measurement. PDP curves were scanned from ± 1mV *vs.* open circuit potential (OCP), at the scan rate of 1 mVs^{-1}. EIS measurements were carried out by running the FRA-2 (frequency response analyzer) module, in a frequency range from 100 MHz to 100 mHz, at steady OCP, with an amplitude of 10 mV ac sine wave. Impedance data for the Cu surface, without and with GO and GO + 4-NBT (0.05 and 0.1 mM), in 0.1 M Na_2SO_4 and 1 M HCl, were recorded in the form of Nyquist plots.

Results and discussion

CV studies

CVs of the pure Cu (99.99%) electrode were recorded in the potential range from -1.2 to +0.8V, in 0.1 M Na_2SO_4 and 1 M HCl, as shown in Fig. 2. In 0.1 M Na_2SO_4, no anodic peak was observed up to 0.0 V, but there was a drastic increase in the current, as indicated in Fig. 2a. The sudden increase in

anodic currents was due to Cu corrosion, and, in the reverse scan, a cathodic peak was observed, which may correspond to $CuCl^-_2$ and CuCl reduction. However, in the 1 M HCl solution, two anodic and one cathodic peak were observed for the bare Cu surface (Fig. 2b). The first oxidation peak in the CV plot corresponds to the Cu dissolution into Cu^+. Consequently, the second oxidation peak represents the process of Cu^+ dissolution into soluble Cu^{2+}. In the reserve sweep, $CuCl_2^-$ corrosion product was partially reduced. As a result, Cl^- concentration at the Cu and salt layer interface increased, which led to fast Cu dissolution into Cu^{2+} [19]. In both 0.1 M Na_2SO_4 and 1 M HCl aggressive media, most of the Cu surface was tarnished, which indicates that general corrosion took place. However, in sulphate (SO_4^{2-}) with electrolytes, a comparatively higher density of pits than that of chloride (Cl-) with electrolytes has been observed [20, 21], at the material surface. Therefore, SO_4^{2-} in a solution was considered more corrosive than the Cl-one.

From the CV responses, without and with GO and GO-4-NBT (0.05 mM and 0.1 mM), it was observed that GO deposition onto the substrate caused a decrease in the hysteresis loop, and that the cathodic current density decreased in 0.1 M Na_2SO_4, while, in the case of 1 M HCl, a small decrease in the height of both anodic and cathodic peaks was observed (Fig. 2).

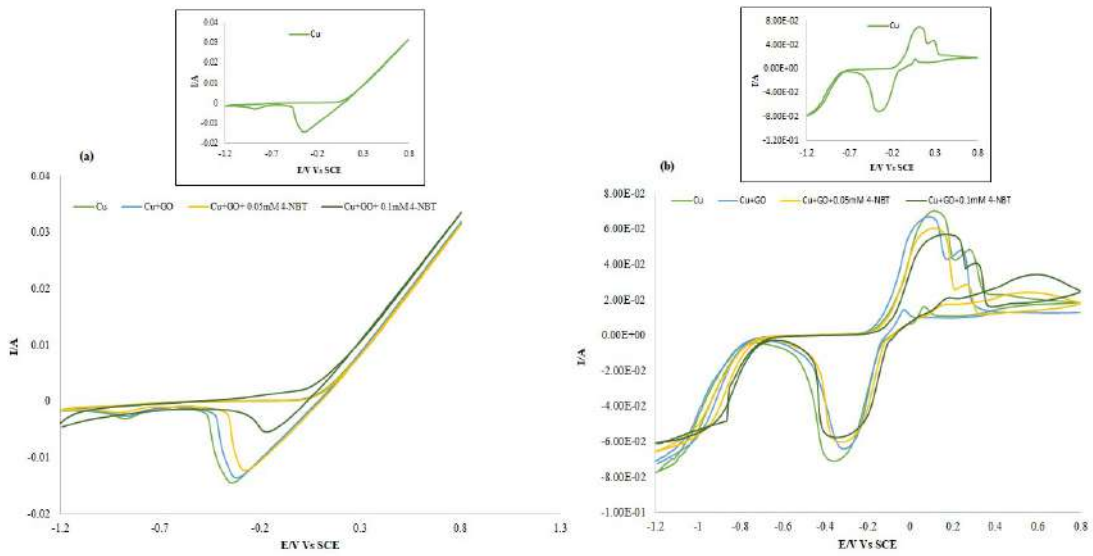

Figure 2. CV responses of the Cu-surface, with and without GO and GO-4NBT in **(a)** 0.1 M Na_2SO_4 and **(b)** 1 M HCl, at a scan rate of 50 mV s^{-1}. The in-set represents CVs of bare Cu in the two aggressive media.

These responses indicate an improvement in Cu corrosion resistance, as GO prevented the aggressive ions from reaching the metal surface in both media [22, 23]. With GO-4-NBT, the current density of the cathodic peak further decreased to a certain extent, which indicates that its presence inhibited the Cu (I) oxidation into soluble Cu^{2+}. The results show that GO-4-NBT is an effective Cu dissolution inhibitor in both media. However, in 1 M HCl, the drop in the current density of both anodic and cathodic

peaks was lower than that in Na_2SO_4, which indicated that the Cu surface in 1 M HCl was not completely covered by a protective layer of GO-4-NBT. Additionally, the extent of inhibition was more pronounced in Na_2SO_4, which could be related to the pits greater density in this medium. GO-4-NBT reduced more effectively the metal surface roughness and filled more evenly these pits in Na_2SO_4 than in HCl.

PDP measurements

PDP curves for Cu in 0.1 M Na_2SO_4 and 1 M HCl, without and with GO and GO-4-NBT (0.05 mM and 0.1 mM), are provided in Figs. 3 and 4, and their parameters are given in Table 1.

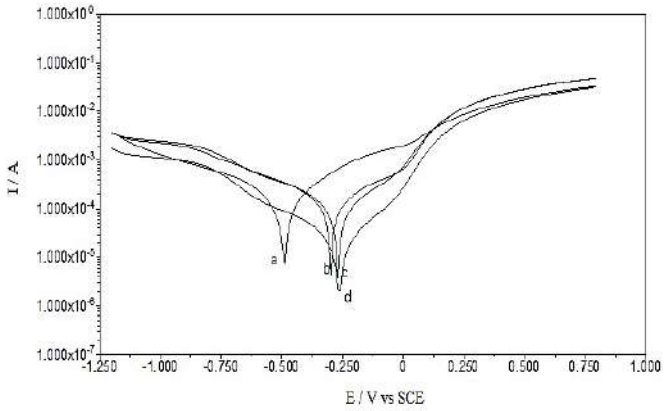

Figure 3. PDP curves of the Cu-surface, with and without GO and GO-4-NBT, in 0.1 M Na_2SO_4.

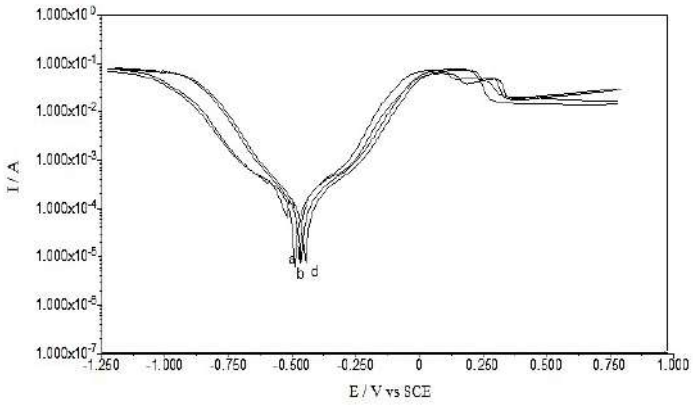

Figure 4. PDP curves of the Cu-surface, with and without GO and GO-4-NBT, in 1 M HCl.

All the scans have exhibited a slightly similar polarization behavior, as shown in Figs. 3 and 4, and indicated no changes in the electrochemical reactions, before and after the inhibitor adsorption onto the Cu surface. The data indicated no significant change in the anodic and cathodic Tafel slopes (β_a and β_c) values, after the inhibitors addition, which revealed that GO and GO-4-NBT did not modify the reaction mechanism. The inhibitors molecules (GO and GO-4-NBT) were adsorbed simply

by blocking the active sites available for reaction. Further, both anodic and cathodic reactions were suppressed after the inhibitors adsorption, while the actual reaction mechanism remained unaffected [24].

Table 1. Potentiodynamic polarization parameters of the Cu surface, before and after the compounds addition at various concentrations, in 0.1 M Na_2SO_4 and in 1 M HCl.

Sample	Medium	Conc. ($M \times 10^{-3}$)	$i_{corr} \times 10^{-4}$ (μAcm^{-2})	$R_p \times 10^4$ (Ωcm^2)	E_{corr} (V vs. SCl	β_c ($Vdec^{-1}$)	β_a ($Vdec^{-1}$)	E_{PDP} %
Cu	0.1 M Na_2SO_4	0.00	0.53	432.7	0.49	0.10	0.11	-
GO		0.002	0.06	808.7	0.30	0.11	0.11	88.67
GO-4-NBT		0.05	0.05	968.1	0.27	0.11	0.11	90.56
GO-4-NBT		0.10	0.04	1025	0.25	0.10	0.11	92.46
Cu	1 M HCl	0.00	0.73	196.4	0.46	0.16	0.13	-
GO		0.002	0.29	205.6	0.44	0.13	0.17	60.27
GO-4-NBT		0.05	0.23	214.0	0.43	0.13	0.16	68.49
GO-4-NBT		0.10	0.18	233.9	0.41	0.12	0.12	75.34

A compound can be classified as an anodic or cathodic-type inhibitor based on the E_{corr} value shift. If the displacement in E_{corr} is greater than 85 mV towards the anode or cathode, with reference to the blank, an inhibitor is categorized as either an anodic or cathodic-type inhibitor, respectively. Otherwise, the inhibitor is treated as a mixed type [25].

The E_{corr} value for the bare Cu surface in 0.1 M Na_2SO_4 was -0.49 mV, but, after GO adsorption, the value shifted to -0.30 mV. After the addition of 0.05 and 0.1 mM 4-NBT, E_{corr} further shifted to -0.27 and -0.25, respectively. Hence, there was a significant change in E_{corr} value, and its maximum displacement was > 85 mV towards a positive potential, indicating that these compounds (GO-4-NBT) are anodic inhibitors. Similarly, in 1 M HCl, the recorded E_{corr} value for the bare Cu surface was -0.460 mV, but it further shifted to -0.440 mV and 0.420 mV, with GO and GO-4-NBT, respectively. The anodic shift in E_{corr} was lower in the HCl medium than in the Na_2SO_4 medium.

A pronounced decrease in Cu i_{corr}, from 0.53×10^{-4} μcm^{-2} to 0.06×10^{-4} μcm^{-2}, with GO, was observed, which was further reduced to 0.05×10^{-4} μcm^{-2} and 0.04×10^{-4} μcm^{-2}, respectively, with GO-4-NBT (0.05 mM and 0.1 mM). A decrease in the corrosion current density (i_{corr}) suggested that both GO and GO-4-NBT inhibited the corrosion process on the Cu surface, by backing off the charge transfer process responsible for dissolution. The polarization resistance value, R_p, increased significantly with higher GO-4-NBT concentrations, which indicates that its action on the Cu surface was efficient.

The corrosion inhibition efficiency (E_{PDP}%) of GO-4-NBT was evaluated from corrosion current densities, by using the following equation:

$$E_{PDP}\% = \frac{i_{corr} - i'_{corr}}{i_{corr}} \times 100 \qquad (1)$$

where i_{corr} and i'_{corr} are the corrosion current densities without and with inhibitors, respectively.

IE for GO, in 0.1 M Na_2SO_4, was 88.67%, suggesting the inhibitor application as a corrosion resistant coating, and, for GO-4-NBT, it was 90.57% (0.05 mM) and 92.46%, (0.1 mM), indicating that the former is better than the latter. Similarly, in 1 M HCl, the IE for the GO coating was 60.27 %, and, for GO-4-NBT, it was 68.49% (0.05 mM) and 75.34% (0.1 mM), respectively. 4-NBT has further enhanced GO IE in both media, despite its values being lower in 1 M HCl.

Adsorption studies

The GO and GO-4-NBT adsorption at a Cu/solution interface can be presented as a substitution adsorption process between the inhibitors molecules in aqueous solutions and the water molecules on a metallic surface. This substitution reaction is written as follows:

$$Org_{(aq)} + nH_2O_{(ads)} \leftrightarrow Org_{(ads)} + nH_2O_{(aq)} \qquad (2)$$

where $Org_{(aq)}$ represents the inhibitor molecules in the aqueous solution, H_2O_{ads} are the adsorbed water molecules onto the metal surface, and n is the number of water molecules removed from the metal surface by each adsorbed inhibitor molecule.

The adsorption nature of a compound can be identified by fitting experimental data into various adsorption isotherms [26]. In the present study, adsorption parameters were found best fitted into the Langmuir's isotherm. The surface coverage (θ) parameter was evaluated using Cu anodic current density without inhibitor, $(I_a)_o$, and with it, $(I_a)_i$, at the concentration indicated in Eq. 3. θ was further used in Eq. 4 to calculate the adsorption constant, K_{ads}, of which values are given in Table 2:

Table 2. Compounds adsorption parameters onto the Cu surface in 0.1 M Na_2SO_4 and 1 M HCl.

Sample	pH	Conc. ($M \times 10^{-3}$)	θ%	C_i/θ ($M \times 10^{-3}$)	K_{ads} ($M^{-1} \times 10^{-3}$)	R_L (V dec-1)	ΔG^0_{ads} ($kJmol^{-1}$)
Cu	0.1 M Na_2SO_4	0.00	-	-		-	
GO		0.002	88.67	0.001		0.292	
GO-4-NBT			0.05	90.56	0.055	2.5	0.008
GO-4-NBT			0.10	92.45	0.108		0.004
Cu	1 M HCl	0.00	-	-		-	
GO		0.002	60.27	0.003		0.720	
GO-4-NBT		0.05	68.49	0.070	0.4	0.048	-25.13
GO-4-NBT		0.10	75.34	0.130		0.024	

$$\theta\% = \left[1 - \frac{(I_a)_i}{(I_a)_o}\right] \times 100 \qquad (3)$$

$$\frac{C_{inh}}{\theta} = C_{inh} + \frac{1}{K_{ads}} \times 100 \qquad (4)$$

A plot of C_{inh} / θ vs. C_{inh} showed a linear regression with its coefficient value, R^2, (0.999 in 0.1 M Na_2SO_4 and 0.997 in 1 M HCl), as shown in Fig. 5.

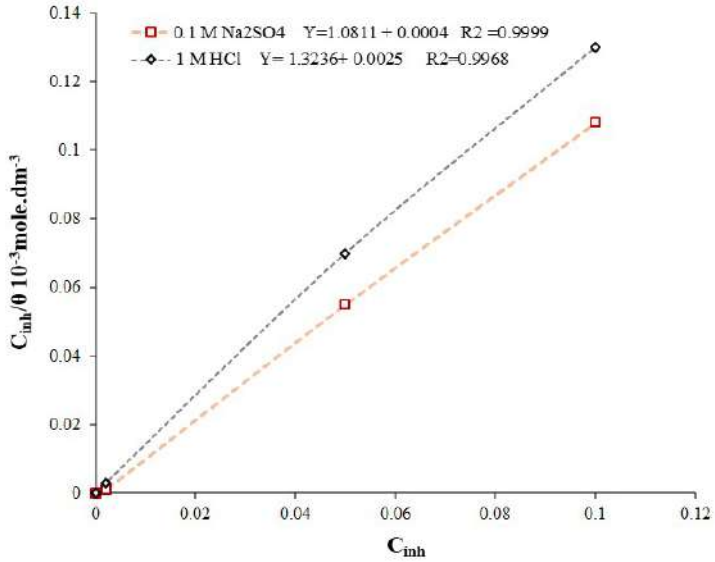

Figure 5. Langmuir's isotherm for GO and GO-4-NBT in 0.1 M Na_2SO_4 and 1 M HCl.

The intercept of the plot enabled to calculate K_{ads} value. The degree of the adsorption process was calculated with the help of Gibb's free energy change (ΔG^0_{ads}), by using K_{ads} value in Eq. 5 [27].

$$K_{ads} = \frac{1}{C_{solvent}} \times e^{-\Delta G^{o}_{ads}} \qquad (5)$$

ΔG^o_{ads} values in both media were > -20 kJ mol^{-1} (Table 2), which indicates the possibility of both electrostatic (physisorption) and coordinated covalent bonding (chemisorption) interactions between the charge metal and the charged inhibitor molecule [26, 28-30].

However, more negative ΔG^o_{ads} values pointed towards a comparatively stronger GO-4-NBT adsorption onto the Cu surface in 0.1 M Na_2SO_4. The dimensionless separation factor (R_L) provides useful data on the feasibility of the inhibitor adsorption. R_L was evaluated by using K_{ads} value in Eq. 6.

$$R_L = \frac{1}{1+K_{ads}C_i} \qquad (6)$$

The values were calculated as lower than 1 (R_L <1) in both aggressive media, which indicates that the inhibitor adsorption process was favorable [31] (Table 2). A pronounced decrease in R_L values was observed with GO. The value approached more zero as 4-NBT concentration was increased. This trend reveals that the inhibitor has covered a wider Cu area, which protected the metal from corrosion, by limiting the charge transfer process.

EIS studies

EIS technique has been used effectively to investigate the corrosion kinetics, and to understand the compounds inhibition mechanism on the metal surface. Impedance

spectra of the Cu electrode in both aggressive media, without and with GO and GO-4-NBT at different concentrations, at OCP, are shown in Fig. 6a and b, in the form of Nyquist plots.

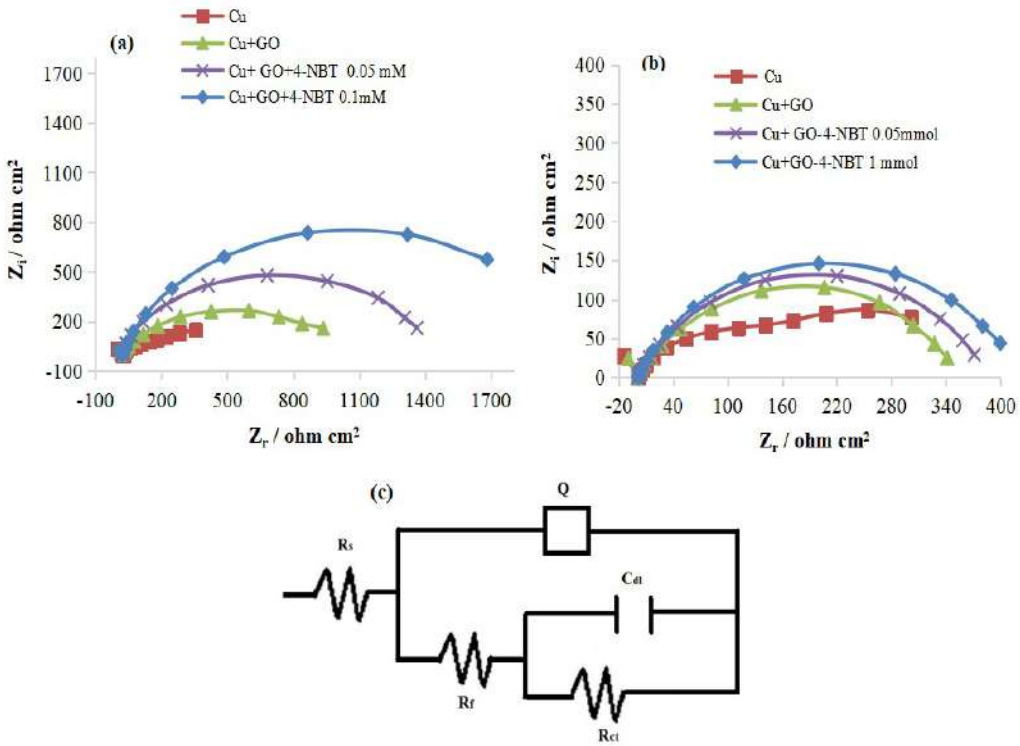

Figure 6. Nyquist plots of the Cu-surface, at OCP, without and with GO and GO-4-NBT (0.05 Mm and 0.1 Mm) in **(a)** 0.1 M Na_2SO_4 and **(b)** in 1 M HCl. **(c)** Equivalent circuit topology used to fit the obtained impedance spectra.

In a Nyquist plot, an imaginary impedance component (Z″) was plotted against the real impedance component (Z′), at each excitation frequency [32]. Thus, the inhibitors effect on the metal/alloy surface could be recognized by the increase in the semicircle diameter, due to a higher resistivity [33]. The semicircle represents the charge transfer at the electrode-electrolyte interface.

Impedance responses obtained without GO and with GO-4-NBT, at various concentrations, showed only one high frequency capacitive loop that indicated charge transfer in the corrosion process, as well as the formation of an oxide layer. For both cases, the capacitive loop and low frequency resistive regions of the impedance shifted to higher values. Consequently, the semicircle increased widely in diameter, which ascribed Cu resistance towards polarization, through the interaction and formation of the inhibitor protecting layers on the metal surface. After GO addition, the hindrance of both mass and charge transfer was improved, which was further reinforced by GO-4-NBT [30]. An equivalent circuit model was used to fit the impedance plots. The circuit topology fit for the experimental

impedance data, in the present study, was proposed as $R_s(R_f–Q[R_{ct}–C_{dl}])$ (Fig. 6c). In the proposed topology, R_s indicates the solution resistance, R_f–Q (high frequency circuit) represents the capacitance and resistance of the surface compact oxide layer and R_{ct}–C_{dl} (medium frequency circuit) corresponds to the charge transfer resistance and double layer capacitance.

The theoretical data using the frequency dependent constant phase element, Q(CPE), fit well with experimental data in the present study. Q(CPE) impedance is given by the following equation:

$$Z_{CPE} = A^{-1}(I\omega)^{-n} \quad (7)$$

where A is the proportional factor, ω is the angular frequency (rad s^{-1}), I ($i^2 = -1$) is an imaginary number and CPE exponent, and n was used to determine the metal surface roughness and inhomogeneity. The CPE type is often used to evaluate data for electrodes with a rough surface [34]. The electrode rough surface might have demobilized the frequency, which, as a result, caused a depression in the semicircle, as well as instability in the data [34]. The exponent (n) greater value represents the surface smoothness and high homogeneity, but, in contrast, a low n value indicates the ions and solvent permeability in the surface.

The fit and calculated parameters are shown in Table 3. It can be observed from the data that R_{ct} increased, while the corresponding C_{dl} values decreased with higher GO-4-NBT concentrations, which reveals that the charge transfer process slowed down, due to the formation of a robust protective layer. The fall in C_{dl} showed the decrease in the dielectric constant, and the increase in the double layer thickness, which further suggested the GO-4-NBT adsorption onto the Cu-solution interface [35]. An increase in n values with higher compounds concentrations indicated that the redox process at low frequencies was not due to the dissolved oxygen diffusion or reduction, but to the inhibitor molecules accumulation at the electrode surface, raising its homogeneity (Table 3).

Table 3. Impedance parameters for the Cu-surface, without and with GO and GO-4-NBT, at different concentrations, in 0.1 M Na_2SO_4 and 1 M HCl.

Sample	Medium	Conc. ($M \times 10^{-3}$)	R_s (Ωcm^2)	R_f (Ωcm^2)	$Q \times 10^{-4}$ ($\Omega^{-1}cm^{-2}sn$)	n	R_{ct} (Ωcm^2)	C_{dl} (μF)	R_T (R_f+ R_{ct})	E_{EIS} (%)
Cu	0.1 M Na_2SO_4	0.00	18.92	9.61	12.91	0.57	81.92	192.60	91.53	-
GO		0.002	19.03	17.14	7.54	0.68	241.46	163.14	258.6	64.60
4-NBT		0.05	19.40	28.11	2.54	0.82	449.29	149.25	477.4	80.82
4-NBT		0.10	21.80	40.35	1.29	0.81	834.25	125.83	874.6	90.00
Cu	1 M HCl	0.00	0.80	2.53	53.34	0.44	55.62	126.41	58.15	-
GO		0.002	0.80	5.94	45.75	0.47	109.26	119.83	115.20	52.0
4-NBT		0.05	0.88	8.17	42.10	0.46	226.7	113.67	121.73	55.23
4-NBT		0.10	0.96	11.62	39.37	0.48	248.4	106.22	136.20	60.66

The corrosion IE% of the compounds can be calculated by using the total resistance data in the following equation:

$$E_{EIS}\% = \left[\frac{(R_T)_i - (R_T)_o}{(R_T)_i}\right] \times 100 \quad (8)$$

where R_T is the total resistance ($R_T = R_f + R_{ct}$) and the subscripts 'i' and 'o' represent the inhibitor presence and absence, respectively. IE for GO was found greater in 0. 1 M Na_2SO_4 then in 1 M HCl, and, for GO-4-NBT (0.1 Mm), it increased up to 90%. IE%, obtained either from corrosion current densities in PDP or from R_T values in EIS, showed similar trends, and a verified considerable improvement for GO-4-NBT in 0.1 M Na_2SO_4.

Conclusions

GO and GO-4-NBT corrosion protection activity was analyzed on the Cu surface in 0.1 M Na_2SO_4 and 1.0 M HCl, by using CV, PDP and EIS. Both anodic and cathodic current in Cu CV response changed with the GO-4-NBT coating, proving it as a mixed type inhibitor. PDP studies showed that GO-4-NBT was adsorbed simply by blocking the active sites available for reaction. Further, both anodic and cathodic reactions were suppressed after the inhibitor adsorption, while the actual reaction mechanism remained unaffected. In EIS studies, the electrode process followed a similar circuit topology, and it was found charged transfer controlled, without and with coated GO and GO-4-NBT. Both PDP and EIS data inferred that the corrosion protection was dependent on the inhibitor concentration, following a spontaneous chemisorption mechanism in both aggressive media. Since SO_4^{2-} in electrolytes was considered more corrosive than Cl-, GO-4-NBT reduced more Cu surface roughness in 0.1 M Na_2SO_4 than in 1 M HCl. Based on these findings, we assure that such studies would help to explore more efficient and cost-effective protective coatings on metal/alloy surfaces that could be used in various industrial applications, especially in the industries where metals are directly exposed to aggressive media.

Acknowledgments

The authors would like to thank the Chemistry Departments of Allama Iqbal Open University for the assistance in carrying out the experimental work.

Conflict of interest

The authors would like to declare that there is no established conflict of interest.

Authors' contribution

Nasima Arshad: conceived and designed the analysis; wrote the paper. **Muhammad Imran**: did the experimental work; performed the analysis. **Muhammad Akram**: helped in the analysis. **Fouzia Altaf**: helped in the analysis.

References

1. Singh BP, Nayak S, Nanda KK, et al. The production of a corrosion resistant graphene reinforced composite coating on Cu by electrophoretic deposition. Carbon. 2013;61:47-56. DOI: https://doi.org/10.1016/j.carbon.2013.04.063

2. Cascalheira AC, Aeiyach S, Lacaze PC, et al. Electrochemical synthesis and redox behaviour of polypyrrole coatings on Cu in salicylate aqueous solution. Electrochim Acta. 2003;48: 2523-2529. DOI: https://doi.org/10.1016/s0013-4686(03)00295-0
3. Tan ALK, Soutar AM. Hybrid sol-gel coatings for corrosion protection of Cu. Thin Solid Films. 2008;516(16):5706-5709. Doi: https://doi.org/10.1016/j.tsf.2007.07.066
4. Schriver M, Regan W, Gannett WJ, et al. Graphene as a long-term metal oxidation barrier: worse than nothing. ACS Nano. 2013;7(7):5763-5768. DOI: https://doi.org/10.1021/nn4014356
5. Lapeire L, Lombardia EM, De Graeve I, et al. Influence of grain size on the electrochemical behavior of pure Cu. J Mater Sci. 2017;52(3):1501-1510. DOI: https://doi.org/10.1007/s10853-016-0445-z
6. Singh AK, Thakur S, Panic B, et al. Green synthesis and corrosion inhibition study of 2-amino-N′-((thiophen-2-yl) methylene)benzohydrazide. New J Chem. 2018;42:2113-2124. DOI: https://doi.org/10.1039/C7NJ04162D
7. Chugh B, Singh AK, Chaouiki A, et al. A comprehensive study about anti-corrosion behaviour of pyrazine carbohydrazide: Gravimetric, electrochemical, surface and theoretical study. J Mol Liq. 2020;299:112160. DOI: https://doi.org/10.1016/j.molliq.2019.112160
8. Singh AK, Quraishi MA. Effect of Cefazolin on the corrosion of mild steel in HCl solution. Corros Sci. 2010;52(1):152-160. DOI: https://doi.org/10.1016/j.corsci.2009.08.050
9. Chugh B, Singh AK, Thakur S, et al. An exploration about the interaction of mild steel with hydrochloric acid in the presence of N-(Benzo [d] thiazole-2-yl)-1-phenylethan-1-imines. J Phys Chem C. 2019;123(37):22897-22917 DOI: https://doi.org/10.1021/acs.jpcc.9b03994
10. Chugh B, Singh AK, Poddar D, et al. Relation of degree of substitution and metal protecting ability of cinnamaldehyde modified chitosan. Carbohydr Polym. 2020;234:115945. DOI: https://doi.org/10.1016/j.carbpol.2020.115945
11. Huh JH, Kim SH, Chu JH, et al. Enhancement of seawater corrosion resistance in Cu using acetone-derived graphene coating. Nanoscale. 2014;6(8):4379-86. DOI: https://doi.10.org/1039/C3NR05997A
12. Chang ML, Cheng TC, Lin MC, et al. Improvement of oxidation resistance of Cu by atomic layer deposition. Appl Surf Sci. 2012;258(24):10128-34. DOI: https://doi.org/10.1016/j.apsusc.2012.06.090
13. Inagaki M. Carbon coating for enhancing the functionalities of materials. Carbon. 2012;50(9):3247-66. DOI: https://doi.org/10.1016/j.carbon.2011.11.045
14. Li X, Cai W, An J, et al. Large-area synthesis of high-quality and uniform graphene films on Cu foils. Science. 2009;324(5932):1312-4. DOI: https://doi.org/10.1126/science.1171245
15. Bae S, Kim H, Lee Y, et al. Roll-to-roll production of 30-inch graphene films for transparent electrodes. Nat Nanotechnol. 2010;5(8):574-8. DOI: https://doi.org/10.1038/nnano.2010.132

16. Nair RR, Blake P, Grigorenko AN, et al. Fine structure constant defines visual transparency of graphene. Science. 2008;320(5881):1308-1308. DOI: https://doi.10.1126/science.1156965
17. Perera SD, Mariano RG, Vu K, et al. Hydrothermal synthesis of graphene-TiO2 nanotube composites with enhanced photocatalytic activity. ACS Catal. 2012;2(6):949-56. DOI: https://doi.org/10.1021/cs200621c
18. Sherif ES, Erasmus RM, Comins JD. Effects of 3-amino-1, 2, 4-triazole on the inhibition of Cu corrosion in acidic chloride solutions. J Colloid Interface Sci. 2007;311(1):144-51. DOI: https://doi.org/10.1016/j.jcis.2007.02.064
19. Kear G, Barker BD, Walsh FC. Electrochemical corrosion of unalloyed Cu in chloride media—a critical review. Corros Sci. 2004;46(1):109-35. DOI: https://doi.org/10.1016/S0010-938X(02)00257-3
20. Souissi N, Triki E. Modelling of phosphate inhibition of Cu corrosion in aqueous chloride and sulphate media. Corros Sci. 2008;50(1):231-41. DOI: https://doi.org/10.1016/j.corsci.2007.06.022
21. Souissi N, Triki E. A chemiometric approach for phosphate inhibition of Cu corrosion in aqueous media. J Mater Sci. 2007;42(9):3259-65. DOI: https://doi.org/10.1007/s10853-006-0809-x
22. Merisalu M, Kahro T, Kozlova J, et al. Graphene–polypyrrole thin hybrid corrosion resistant coatings for Cu. Synth Met. 2015;200:16-23. DOI: https://doi.org/10.1016/j.synthmet.2014.12.024
23. Abd El-Maksoud SA, Fouda AS. Some pyridine derivatives as corrosion inhibitors for carbon steel in acidic medium. Mater Chem Phys. 2005;93(1):84-90. DOI: https://doi.org/10.1016/j.matchemphys.2005.02.020
24. Arshad N, Singh AK, Akram M, et al. Experimental, theoretical, and surface study for corrosion inhibition of mild steel in 1 M HCl by using synthetic anti-biotic derivatives. Ionics. 2019:25:5057-5075. DOI: https://doi.org/10.1007/s11581-019-03028-y
25. Verma C, Quraishi MA, Kluza K, et al. Corrosion inhibition of mild steel in 1 M HCl by D-glucose derivatives of dihydropyrido [2,3-d:6,5-d′] dipyrimidine-2, 4, 6, 8(1H,3H, 5H,7H)-tetraone. Sci Rep. 2017;7:1-17. DOI: https://doi.org/10.1038/srep44432
26. Myung NV, Park DY, Yoo BY, et al. Development of electroplated magnetic materials for MEMS. J Magn Mater. 2003;265(2):189-198. DOI: https://doi.org/10.1016/S0304-8853(03)00264-6
27. Arshad N, Akram AR, Akram M, et al. Triazolothiadiazine derivatives as corrosion inhibitors for Cu, mild steel and aluminum surfaces: Electrochemical and quantum investigations. Prot Met Phys Chem Surf. 2017;53:343-358. DOI: https://doi.org/10.1134/S2070205117020046
28. Sherine HB, Rajendran S. Corrosion inhibition of carbon steel in ground water by thiophenol-Zn^{2+} system. Arab J Sci Eng. 2011;36:517-528. DOI: https://doi.org/10.1007/s13369-011-0067-3
29. Saji VS. A review on recent patents in corrosion inhibitors. Recent Patents. Corros Sci. 2010;2:6-12. DOI: https://doi.org/10.2174/1877610801002010006

30. Amin MT, Alazba AA, Shafiq M. Adsorptive Removal of Reactive Black 5 from Wastewater Using Bentonite Clay: Isotherms, Kinetics and Thermodynamics. Sustainability. 2015;7(11):15302-15318. DOI: https://doi.org/10.3390/su71115302
31. Tiginyanu I, Topala P, Ursaki V. Book: Nanostructures and Thin Films for Multifunctional Applications. Technology, Properties and Devices. Springer International Publishing Switzerland 2016; Ed. 1: 576 pages. DOI: https://doi.org/10.1007/978-3-319-30198-3.
32. Rbaa M, Galai M, El-Faydy M. Synthesis and Characterization of New Benzimidazoles Derivatives of 8-hydroxyquinoline as a Corrosion Inhibitor for Mild Steel in 1.0 M Hydrochloric Acid Medium. Analyt Bioanalyt Electrochem. 2017;9(7):904-928. www.abechem.com
33. Jorcin JB, Orazem ME, Pébère N, et al. CPE analysis by local electrochemical impedance spectroscopy. Electrochim Acta. 2006;51(8-9):1473-1479. DOI: https://doi.org/10.1016/j.electacta.2005.02.128
34. Li G, Ma H, Jiao Y, et al. An impedance investigation of corrosion protection of Cu by self-assembled monolayers of alkanethiols in aqueous solution. J Serbian Chem Soc. 2004;69:791-805. DOI: https://doi.org/10.2298/JSC0410791L
35. Arshad N, Altaf F, Akram M, et al. Furan and Phenyl Substituted Triazolothiadiazine Derivatives as Cu Corrosion Inhibitors: Electrochemical and DFT Studies. Prot Met Phys Chem Surf. 2019;55(4):770-780. DOI: https://doi.org/ 10.1134/S2070205119040038